Soils and Rocks
An International Journal of Geotechnical and Geoenvironmental Engineering
www.soilsandrocks.com
ISSN 1980-9743
ISSN-e 2675-5475

Effect of weathering on the stability of rock slope at a water intake canal of Simplicio Hydroelectric Power Plant

Patrícia Martins Lopes[1#], Alberto de Sampaio Ferraz Jardim Sayão[1],
Anna Laura Lopes da Silva Nunes[2]

Case Study

Keywords
Alterability
Rock and joint behavior
Slope stability analysis

Abstract

Rock and joint alteration leads to modifications in their properties, resulting in a reduction of rock mass strength and consequently a decrease in the safety of engineering structures. The alteration process changes the material and alters its geomechanical behavior. This research presents the studies conducted to evaluate the mechanical behavior of rock joints in the gneiss massifs that make up the hydraulic circuit of the Simplicio Hydroelectric Plant due to their alteration. Compilation and analysis of data from previous research were carried out to parameterize the joints at different levels of alteration. Deterministic stability analyses showed that the alteration process of gneiss joints can significantly reduce the slope safety factor by up to half of its initial value. Furthermore, probabilistic analyses revealed an increase in failure probability of approximately 10% among the studied alteration classes. The results underscore the importance of assessing the level of joint alteration in engineering projects.

1. Introduction

The alteration of rock materials results from their exposure to weathering agents, thus being the effect of a geological process. Physical and chemical changes induced by this exposure can modify the engineering properties of rock masses, leading to their weakening due to the appearance of fissures, mineral alterations, and a reduction in material strength (Guidicini & Nieble, 1983; Teixeira et al., 2000; Maia, 2001; Maia et al., 2002, 2003; Press et al., 2006).

The alteration of rocks and their discontinuities may lead to a decrease in material strength and deformability, together with block disintegration and increased permeability. Understanding this process enables the prediction of the behavior of rock masses over time, thus enabling the valuation of the required time for maintenance and preventive actions.

Thus, the present study seeks to assess the influence of gneiss joint alteration on the mechanical behavior of a water canal at the Simplicio Hydroelectric Power Plant (AHE Simplicio). It is part of a series of investigations carried out over the past two decades by the Alterability Research Group at PUC-Rio and COPPE-UFRJ.

Among the previous research conducted by the group, notable works include those by Maia (2001), Maia et al. (2002, 2003) on the rock masses of the Marimbondo and Serra da Mesa dams, in Brazil, as well as the research conducted on the rock masses of the Simplicio Hydroelectric Project by Machado (2012), Salles (2013), Oliveira (2017), Steffens (2018), Lopes (2019) and Lopes (2023). These studies were conducted following recurrent failures during the excavation of the gneissic canal slopes at the Simplicio Hydroelectric Power Plant. This research aimed at assessing the influence of altered rock on the stability both rock and residual soil slopes.

The compilation and comprehensive analysis of the results from the previous research, particularly those by Oliveira (2017), Steffens (2018), and Lopes (2019), served as a basis for defining the parameters of rock joints at different levels of alteration. The main objective of the present research is to establish the influence of gneiss alteration on the geotechnical parameters of Simplicio rock which can affect the stability of the water intake canal slopes within the project.

2. Shear strength of joints

Roughness is associated with the morphology of discontinuity walls. This feature of joints, in conjunction with the compressive strength of the walls, can significantly influence the mechanical behavior of the rock mass. However, its importance is reduced as more criteria on joint opening, filling, and degree of prior displacement are considered.

[#]Corresponding author. E-mail address: pathy.malopes@gmail.com
[1]Pontifícia Universidade Católica do Rio de Janeiro (Puc-Rio), Departamento de Engenharia Civil, Rio de Janeiro, RJ, Brasil.
[2]Instituto Alberto Luiz Coimbra de Pós-Graduação e Pesquisa de Engenharia (COPPE - UFRJ), Programa de Engenharia Civil, Rio de Janeiro, RJ, Brasil.

Submitted on October 30, 2023; Final Acceptance on June 27, 2024; Discussion open until February 28, 2025.
https://doi.org/10.28927/SR.2024.010623

Shear strength of joints is directly linked to their roughness, especially in unfilled discontinuities. The magnitude of shear strength of joints is related to the peak or residual friction angle, combined with the contribution of roughness. Patton (1966) proposed a failure criterion that takes into account the influence of this roughness in estimating the strength of discontinuities. Thus, two failure envelopes were proposed, one for low nominal loads (Equation 1), i.e., when there is no shearing of roughness, and another for high nominal loads (Equation 2), when shearing of irregularities occurs, resulting in a reduction in the friction angle.

$$\tau = \sigma_n . tan\left(\phi_b + i\right) \tag{1}$$

$$\tau = c_j + \sigma_n . tan\phi_r \tag{2}$$

where, σ_n = effective normal stress, ϕ_b = basic friction angle, i = average angle of deviation of particle displacements from the direction of the applied shear stress, c_j = cohesion intercept of the joint, ϕ_r = residual friction angle.

Barton (1973) developed a criterion that considers the influence of roughness and the compressive strength of discontinuity walls on the shear strength of rock joints. The criterion accounts for two components of strength: the portion related to the rock mineralogy and the portion linked to discontinuity roughness, as presented in Equation 3.

$$\tau = \sigma_n . \tan\left(JRC . \log\left(\frac{JCS}{\sigma_n}\right) + \phi_b\right) \tag{3}$$

where, JRC = Joint Roughness Coefficient, JCS = Joint Compressive Strength.

The basic friction angle (ϕ_b) represents the portion of the strength associated with the mineralogy of unaltered, dry, and flat joints, meaning those that exhibit no visible roughness components. According to Bandis (1980), the basic friction angle can be determined from the residual shear strength of flat rock surfaces. This parameter can be determined through direct shear tests, tilt tests, and push or pull tests, using sawn or sandblasted surfaces.

Subsequent contributions enhanced the criterion presented by Barton (1973), incorporating additional considerations, such as the use of the residual friction angle (ϕ_r) for altered joints (Barton & Choubey, 1977) and the scale effect (Barton & Bandis, 1982).

The residual friction angle (ϕ_r) was incorporated into the criterion to broaden its applicability to altered saturated joints. This parameter corresponds to the residual friction angle of altered and/or saturated joints. Its determination can be achieved through direct shear tests with sufficiently long displacements to eliminate the effects of joint roughness (Woo et al., 2010). Equation 4 presents the generalized criterion for the shear strength of joints.

$$\tau = \sigma_n . \tan\left(JRC . \log\left(\frac{JCS}{\sigma_n}\right) + \phi_r\right) \tag{4}$$

The residual friction angle (ϕ_r), like the basic friction angle (ϕ_b), depends on the constituent materials of the joint. However, the former also depends on the level of alteration of these materials. Therefore, the level of alteration is one of the most important factors influencing the residual friction angle for rock joints with the same mineralogy and grain size (Woo et al., 2010).

The roughness component of the joint depends on three main elements: the joint roughness coefficient (*JRC*), the joint compressive strength of the discontinuity walls (*JCS*), and the acting normal stress on the assembly. Joints with lower roughness are less affected by the value of *JCS*, as roughness has less influence when the joint roughness coefficient (*JRC*) is reduced (Barton, 1978).

According to Kveldsvik et al. (2008), for low-acting normal stresses, joint roughness has a significant impact on assembly strength. This phenomenon is due to joint dilation caused by roughness during shearing. For higher normal stresses, the effect of joint roughness is reduced due to the decrease in the ratio between the joint compressive strength and the acting normal stress (JCS / σ_n).

Most stability problems related to rock slopes occur under low-acting normal stresses. Therefore, roughness is a fundamental component in the study of shear strength for unaltered and unfilled joints (Barton, 1978).

Joint wall compressive strength (*JCS*) was defined by Barton (1973, 1978) as equal to the uniaxial compressive strength of the rock (σ_c) for unaltered joints or as a portion of (σ_c) for altered joints, which can amount to 1/4 of σ_c.

According to Barton (1978), joint wall compressive strength is an essential component of shear strength. Consequently, processes that could reduce this portion, such as alteration and moisture variation, may decrease the shear strength of the assembly.

Joint wall compressive strength (*JCS*) can be estimated through uniaxial compression tests or Schmidt hammer tests (Barton & Choubey, 1977).

Among the parameters involved in the strength criterion defined by Equation 4, the joint roughness coefficient (*JRC*) is the most challenging to determine. Its estimation can be carried out by comparing roughness profiles, measuring roughness, or through testing methods (Leite & Dantas Neto, 2020; Dantas Neto et al., 2022).

Methods for measuring roughness include the use of profilometers, photogrammetry, laser scanning, among others Regarding *JRC* estimation methods through testing, direct shear tests, tilt tests, and push or pull tests can be conducted.

Direct shear tests can be performed on circular or square samples, providing shear stress versus normal stress curves, shear stress versus displacement curves, and dilation versus displacement curves, as outlined in Figure 1 (Barton et al., 2023).

The *JRC* value can be estimated by retro-analyses of the data obtained from the direct shear test of rock joints through the rearrangement of Equation 4.

2.1 Scale effects

JRC and *JCS* values are dependent on the scale of the tested sample. In general, larger blocks tend to have a lower *JRC* value compared to smaller blocks, considering the same rock joint. Barton & Bandis (1982) proposed Equations 5 and 6 to correct the scale effect.

$$JRC_n \approx JRC_o \left(\frac{L_n}{L_o} \right)^{-0.02*JRC_o} \quad (5)$$

$$JCS_n \approx JCS_o \left(\frac{L_n}{L_o} \right)^{-0.03*JRC_o} \quad (6)$$

where, JCS_o = *JCS* measured in the laboratory, L_n = joint in situ length, L_o = joint length in laboratory.

According to Barton & Bandis (1982), the scale effect tends to decrease as the sample dimensions exceed the natural size of blocks found in the field.

Furthermore, the scale effect alters the behavior of the joint in terms of dilation and the required displacement to mobilize peak resistance. Samples with larger dimensions experience reduced dilation during shearing, while the displacement required to mobilize peak resistance increased.

As observed by Goodman (1970), Barton (1973), and Pratt et al. (1974), the peak dilation of joints occurs simultaneously with or shortly after the peak shear resistance of the sample, demonstrating a strong correlation between these quantities.

2.2 Barton-Bandis failure criterion

The shear strength criterion for joints presented earlier is also known as the Barton-Bandis failure criterion. The Barton-Bandis failure criterion has been used over the past decades and provides a reliable approximation for the behavior of unfilled rock joints.

The Barton-Bandis (BB) model is a nonlinear method and is considered more accurate when compared to the linear Mohr-Coulomb (MC) method. Numerous studies have been conducted to assess the effectiveness of applying the BB model to predict shear resistance in joints and the stability of their slopes, with these research efforts yielding favorable results and approximations (Barton et al., 2023).

Barton et al. (2023) emphasize that despite all the advancements achieved, the determination of joint roughness remains complex and continues to be a challenge even today.

3. Stability analysis

The stability of rock slopes is influenced by numerous factors such as stress and drainage conditions, mechanical properties of the massif, and the distribution of discontinuities. In general, the presence of joints represents a zone of weakness in which the properties of these discontinuities govern the stability of the rock mass in terms of shear and deformation (Barton et al., 2023).

According to Barton et al. (2023), there are two primary approaches for evaluating the stability condition of rock slopes, considering the influence and properties of joints: the discontinuous and continuous approaches.

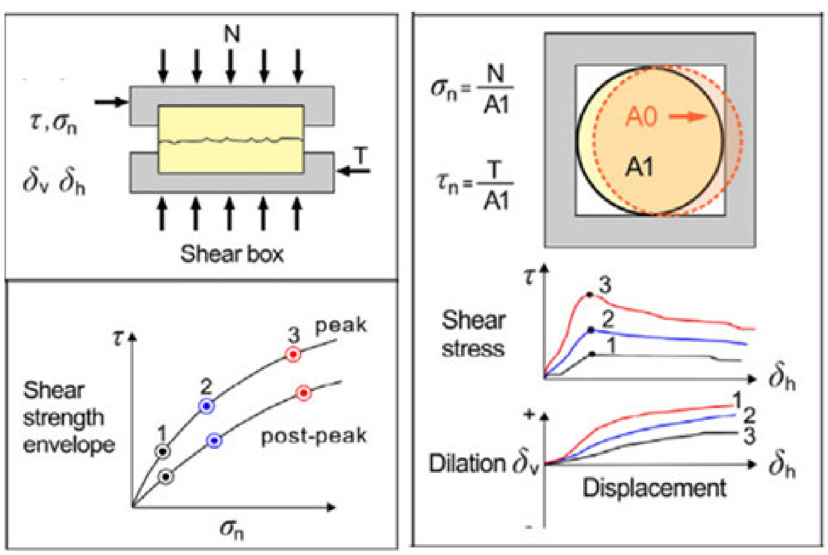

Figure 1. Typical direct shear test results (Barton et al., 2023).

The discontinuous approach models the geological structure within the massif, allowing the present discontinuities to control deformation and failure modes. The continuous approach corresponds to simulating the rock mass as a medium that assumes the properties of the joints, transforming the slope discontinuity into a hypothetical continuous medium.

According to Barton et al. (2023), both approaches are applicable under specific conditions. The discontinuous approach is more appropriate when the geological structure controls anisotropy, deformation, and massif strength. On the other hand, the continuous approach is more suitable when the frequency and orientation of the joints are such that there are no preferential paths of rupture and/or deformation.

Generally, stability analyses in geotechnical engineering are conducted considering deterministic analyses, in which a safety factor is obtained as the ratio of resisting applied forces. In deterministic analyses, the use of average parameters disregards the uncertainties surrounding the stability analyses of a structure or slope, such as strength parameters, site stratigraphy, groundwater level, amongst others.

Probabilistic analyses emerge to account for all these uncertainties, complementing deterministic analyses and providing probability distribution of failure related to each value of the safety factor (*SF*). Thus, it enables the assessment of the distribution of *SF* as a variable dependent on the distribution of various independent variables.

In the probabilistic approach, a variable or performance indicator *y* (*SF*, settlement, flow rate, among others) is described through a mathematical function, whose statistical distribution allows for the calculation of the most probable value and the failure probability associated with each value (Assis et al., 2018).

Probabilistic methods enable the determination of the probability distribution of a dependent variable (performance indicator) based on the statistical distributions of its independent variables. Some of the primary probabilistic methods include the First Order Second Moment (FOSM) and the Monte Carlo Method (MCM).

3.1 First Order Second Moment (FOSM)

The FOSM method was developed as an expansion of the Taylor series of the equation for the variance of a dependent variable *y* in terms of independent random variables, where this expansion is truncated at its first-order terms.

According to Griffiths & Fenton (2007), this method provides approximations for the mean and standard deviation of the dependent variable based on the means and standard deviations of all independent random variables. Therefore, it is not necessary to determine the probability distribution function of the independent variables. In other words, the calculation of failure probability is based solely on the moments of the statistical distribution (mean and standard deviation) of the random variables (Sayão et al., 2012).

Considering $x1$, $x2$, ..., xn as random variables in the calculation of the safety factor (*SF*), the mean value of X and its performance function are represented by X and F(X). The truncated Taylor series for the expansion of the function F(X) around the point $X = \bar{X}$ is given by Equation 7. Equation 8 presents the variance of the safety factor for N random variables.

$$F(X) = f(\bar{X}) + f'(\bar{X})(X - \bar{X}) \tag{7}$$

$$V(F) = \sum_{\mathrm{i}=1}^{N} \left(\frac{\partial SF}{\partial x_i} \right)^2 V(x_i) \tag{8}$$

Christian et al. (1992) introduced a methodology for approximating partial derivatives through a simplification based on the divided differences method. The methodology involves an incremental variation of each parameter defined as a random variable and the corresponding change in the safety factor (*SF*). The approximation of the partial derivative with respect to each parameter is obtained by the ratio of the *SF* variation to the parameter variation, as indicated in Equation 9.

$$\left(\frac{\delta SF}{\delta x_i} \right) = \frac{SF(x_i + \delta x_i) - SF(x_i)}{\delta x_i} \tag{9}$$

3.2 Monte Carlo Method (MCM)

The Monte Carlo Method seeks to find an approximate numerical solution for the probability distribution of the dependent variable by using a technique in which a sequence of random numbers is generated to characterize the function F(X) in a representative manner. As the number of generated values tends to infinity, the result becomes more precise and accurate.

After repeating the calculation process *N* times for all values of the independent variables, a sample of discrete values of the variable F(X) is obtained. This allows for the calculation of its mean, standard deviation, the best-fitting probability distribution, and failure probability.

4. Study area and material

The Simplicio Hydroelectric Power Plant is located between the municipalities of Três Rios (RJ), Sapucaia (RJ), Chiador (MG), and Além Paraíba (MG), extending parallel to the banks of the Paraíba do Sul River (Figure 2). The project consists of the small Anta Hydroelectric Plant (PCH Anta), where the river is dammed, and the Simplicio Hydroelectric Plant (UHE Simplicio). After damming, a portion of the flow is diverted through an intake circuit that

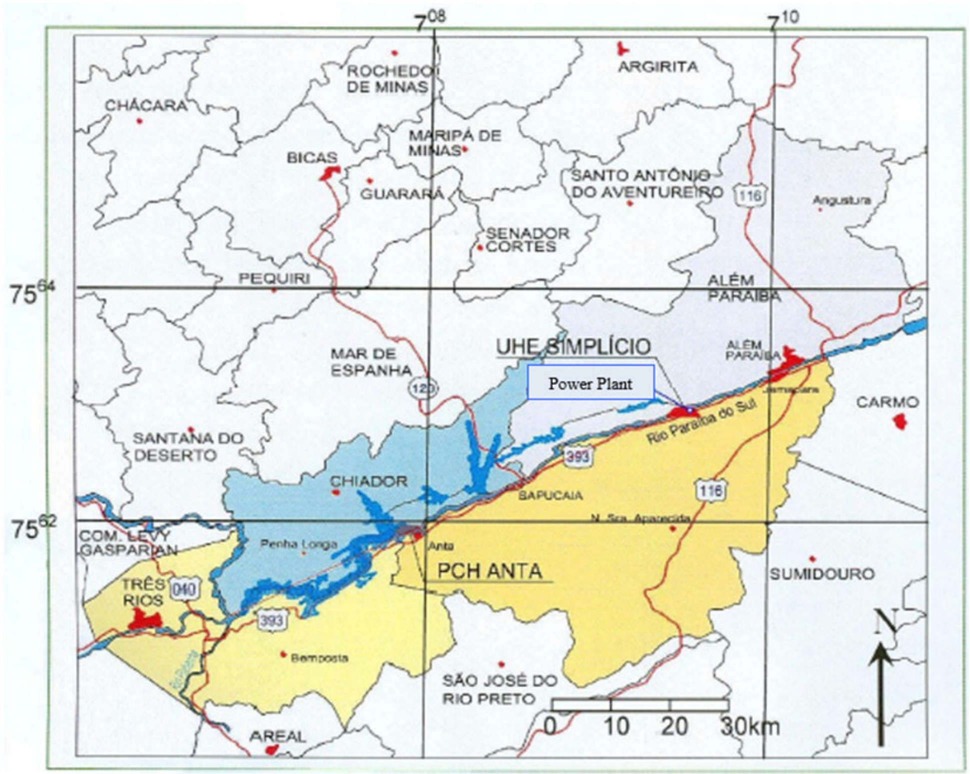

Figure 2. Location of Simplicio Hydroelectric Power Plant (Marchesi, 2008).

spans approximately 30 km and includes canals, tunnels, reservoirs, and dikes.

This circuit is responsible for conveying water to the powerhouse of the UHE Simplicio, where energy generation occurs through a single drop, harnessing a natural elevation difference of 115 meters (Machado, 2012; Steffens, 2018).

The project site is situated within the Além Paraíba Lineament unit, also known as the Paraíba do Sul River Shear Zone, and features high-grade igneous and metamorphic rocks (Dehler & Machado, 2002; Viana, 2010). This shear zone is a transcurrent fault zone characterized by a prominently N60E-aligned topography. The surrounding geology consists of crystalline substrates of gneisses, migmatites, and granitoid rocks intruded by diabase dikes, partially overlain by deposits of alluvial, colluvial, and residual soils (Valeriano, 2006; Marinho, 2007).

Regarding climate, the region experiences a humid climate with annual precipitation exceeding 1200 mm, leading to significant weathering of rocks along fractures, resulting in well-developed weathering mantles that become more susceptible to sliding and erosion (Marinho, 2007).

The samples tested by Oliveira (2017) and Steffens (2018) were obtained from rotary drillings conducted within the project area and tested in the laboratory by Salles (2013). The block samples tested by Lopes (2019) in the laboratory were collected from excavation areas of the project canals, primarily from Canal 1 excavations. These samples were separated and stored in sealed containers, which remained in an open area of the Geotechnical Laboratory of COPPE-UFRJ for 10 years, exposed to weathering agents such as temperature and humidity variations.

5. Definition of geotechnical parameters and geometry

Using Barton's (1973) shear strength criterion for rock joints, as presented in Equation 4, and the results obtained by Steffens (2018) and Lopes (2019) through direct shear tests and Schmidt Hammer tests, along with relevant literature references on the subject, it was possible to determine the geomechanical parameters of the gneiss joints at the Simplicio Hydroelectric Plant (AHE Simplicio) region.

Steffens (2018) assessed the mechanical behavior of the rock joints at the AHE Simplicio for various levels of natural and artificial alteration. This involved conducting direct shear tests and Schmidt Hammer tests on core samples taken from drillings in Canal 1 of the hydropower project, which had been altered in the laboratory by Salles (2013). Salles (2013) subjected the samples to accelerated percolation for various alteration times: 0 hours, 600 hours, 1200 hours, 2400 hours, 4800 hours, and 83000 hours.

Lopes (2019) conducted Schmidt Hammer tests in both field and laboratory settings for different levels of joint alteration and developed a proposal to predict behavior over time for the gneiss in the region of the Simplicio Hydroelectric Project.

According to Barton's (1973) equation for the shear strength of rock joints (Equation 4), the variables to be defined for the use of the Barton-Bandis failure criterion are *JCS*, *JRC*, and the residual friction angle (ϕ_r), in addition to the rock unit weight (γ) and the joint friction angle (ϕ).

To evaluate the influence of the level of joint alteration on the stability of rock masses, the approach chosen was to treat the massif as a hypothetical continuous medium, with joint parameters governing the geomechanical behavior.

Furthermore, five levels of alteration were defined to determine the parameters, encompassing the alteration times presented in Table 1. Subsequently, these levels of alteration will be used to define five stability analysis scenarios.

5.1 Joint Compressive Strength (*JCS*)

Joint Compressive Strength (*JCS*) can be obtained through the Schmidt Hammer test, in which the rebound of the joint surface is measured, and its compressive strength is deduced through correlation.

Based on the results obtained by Steffens (2018) and reevaluated by Lopes (2019), the average *JCS* value for each level of alteration of the laboratory samples (ranging from 0 hours to 8300 hours) can be seen in Table 2.

5.2 Residual friction angle

The residual friction angle of joints can be obtained through direct shear tests and tilt tests, in which unfilled joints are sheared under low stresses (self-weight of the upper part). It can also be derived through correlation with the basic friction angle and the rebound values of the altered joint and the intact rock.

Table 1. Level of alteration defined according to the alteration time.

Level	Weathering Level	Time of alteration
Level 1	Unaltered Joint	Field Test (Fresh Joint)
Level 2	Very Slightly Altered Joint	0 hours of laboratory alteration
Level 3	Slightly Altered Joint	600 hours of laboratory 1200 h of laboratory alteration
Level 4	Moderately Altered Joint	2400 h of laboratory alteration 4800 h of laboratory alteration
Level 5	Moderately Altered Joint	8300 h of laboratory alteration

Table 2. JCS, JRC and unit weight considering the scale effect.

Level	JCS_n (MPa)	JRC_n	γ (kN/m^3)
Level 1	139.3	7.1	27.0
Level 2	46.6	5.8	25.7
Level 3	38.7	5.6	24.3
Level 4	25.1	5.6	21.6
Level 5	19.5	6.4	21.6

Based on the results obtained by Steffens (2018) for flat gneiss joints that were not subjected to accelerated alteration in the laboratory (samples with 0 hours of alteration), a value of ϕ_r equal to 35° was determined.

5.3 Joint Roughness Coefficient (*JRC*)

For the calculation of the joint roughness coefficient, Equation 4 was employed, replacing the shear and normal stress with their peak values, and substituting the basic friction angle with the residual angle, as illustrated in Equation 10.

$$JRC = \frac{\tan^{-1}\left(\frac{\tau_{peak}}{\sigma_{n\,peak}}\right) - \phi_r}{\log\left(\frac{JCS}{\sigma_n}\right)} \tag{10}$$

where, τ_{peak} = peak shear strength, $\sigma_{n_{peak}}$ = effective normal stresss at peak shear strength.

Using Equation 10 and the raw data obtained by Steffens (2018) from direct shear tests on gneiss joints, it was possible to calculate the corresponding *JRC* value for each set of peak shear stress to normal stress. For the unaltered joint tested in the field using the Schmidt Hammer, the *JRC* value was assumed to be the highest *JRC* value found for the samples with 0 hours of laboratory alteration, resulting in *JRC* = 13.3. Therefore, the average *JRC* values for each level of alteration are presented in Table 2.

5.4 Rock unit weight

In this study, the unit weight of unaltered gneiss will be considered as 27 kN/m^3. Using the unit weight reduction ratio proposed by Barton & Choubey (1977), the unit weight values for each level of alteration studied in this research were obtained. The values are presented in Table 2.

5.5 Joint friction angle

Based on the results obtained by Steffens (2018) in the direct shear tests of gneiss joints, it was possible to construct the Mohr-Coulomb strength envelopes to determine the joint friction angle for each laboratory alteration time. The friction angle values obtained for each level of alteration and their respective averages are presented in Table 2. For the unaltered joint tested in the field, the highest friction angle value from the presented envelopes was adopted, which is equal to 37°.

5.6 Field parameters – Scale effect

In order to compare the safety factors obtained by considering the laboratory-tested parameters with the field parameters suggested by Equations 5 and 6, Table 2 presents the field results for *JCS*, *JRC*, and unit weight for each level of alteration. It should be noted that for this study, the block size in the field (L_n) was considered to be equal to 0.5 m.

5.7 Geometry

Due to the impossibility of accessing the geological-geotechnical section of the Simplicio canals, a schematic geometric section was adopted in this work, based on images of Canal 1 excavations and information published by Motta et al. (2009).

According to Motta et al. (2009), part of the slopes of Canals 1, 2, 3, and 4 were built on slopes of 1(V):1.3(H), with a berm height equal to 10 m and a width of 4 m. Furthermore, from images from Channel 1, it was possible to notice that in some points, the three lower banks received rockfill berms, and the others were made up of soil. The lower banks are precisely the gneiss banks that suffered recurrent failures and whose stability needed to be increased through the placement of rockfill berms.

Considering the available information, the schematic geometry of the slopes was considered with a slope of 1(V):1.3(H), with a berm height of 10m and a width of 4m. In order to analyze the influence of the joint behavior on the stability of the massif and how its alteration reduces the safety of the canals, the three lower benches in rock were modeled. In other words, the region of the slopes consisting of residual gneiss soil was not considered in the analyses. The final geometry analyzed is presented in Figure 3.

5.8 Stability analysis scenarios

In this research, the rock mass was modeled as a continuous medium, with parameters based on the geomechanical behavior of intact and/or altered joints in the gneiss of the Simplicio region. Namely, the properties of the joints were assumed to govern the behavior of the rock mass.

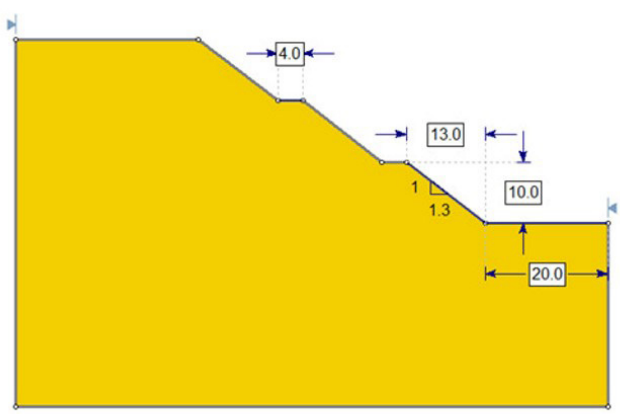

Figure 3. Schematic geometry defined for the stability analyses in this study.

This approach was adopted to understand how joint alteration can influence the stability of the Simplicio canals and other structures with similar material characteristics.

As previously discussed, deterministic and probabilistic stability analyses were conducted using the limit equilibrium approach and the Barton-Bandis failure criterion. Rocscience Slide2 software was used for the analyses, and the safety factors were obtained for non-circular surfaces using the Spencer and Morgenstern-Price methods.

Five scenarios were considered for the analysis of rough joints, with one scenario for each level of alteration defined previously in Table 1. Additionally, for all scenarios, the analyses were conducted both with and without considering the influence of the water level, as presented in Table 3. The standard deviations considered in the probabilistic analyses for each scenario are shown in Table 4.

6. Analysis and results

6.1 Geotechnical parameters

The dispersion of *JRC* values, peak friction angle, and friction angle obtained in the direct shear tests is presented in Figure 4, according to the level of alteration of the samples.

There is a noticeable trend of reduction in both the peak friction angle and the friction angle of the gneiss joints. Additionally, a slight increase in the dispersion of *JRC* values, peak friction angle, and friction angle can be observed as the level of alteration increases.

As depicted in Figure 4, there exists a discernible trend of friction angle reduction as the level of joint alteration escalates. Furthermore, an escalation in result dispersion is noticeable for more substantial levels of alteration. Figure 4 also indicates a tendency towards a decrease in the peak friction angle when considering the average of laboratory-derived values. The *JRC* value experiences a marginal decrease for initial alteration levels and a significant increase at the highest alteration level, along with an escalation in dispersion.

According to Woo et al. (2010), both the peak friction angle and the friction angle tend to diminish as the alteration of granite joints intensifies, while the *JRC* value generally rises. Despite this increase in the joint roughness coefficient, shear resistance tends to be lower for altered joints due to the reduction in other parameters, namely the peak friction angle, friction angle, and *JCS*.

In general, the results presented herein align with the behavior trends described in the literature, with the substantial dispersion and some divergent points attributed to the number of shear tests performed, which is considered below the ideal.

Figure 5 illustrates the graph of peak shear stress and ultimate shear stress against the normal stresses applied during direct shear tests. Additionally, four shear stress trajectories were plotted on the graph using the Barton-Bandis model: two trajectories employing laboratory-derived parameters for intact joints (green trajectory) and highly altered joints

Table 3. Analysis scenarios for rough joints and their respective levels of alteration.

Scenarios	*JCS* (MPa)	*JRC*	γ (kN/m^3)	ϕ (°)	Water level
Scenario 1	139.3	7.1	27	37	-
Scenario 2	46.6	5.8	25.7	35	-
Scenario 3	38.7	5.6	24.3	33	-
Scenario 4	25.1	5.6	21.6	31	-
Scenario 5	19.5	6.4	21.6	27	-
Scenario 6	139.3	7.1	27	37	12 m
Scenario 7	46.6	5.8	25.7	35	12 m
Scenario 8	38.7	5.6	24.3	33	12 m
Scenario 9	25.1	5.6	21.6	31	12 m
Scenario 10	19.5	6.4	21.6	27	12 m

Table 4. Standard deviation considered in the probabilistic analyses for each scenario.

Scenarios	σ_{JCS} (MPa)	σ_{JRC}	σ_{γ} (kN/m^3)	σ_{ϕ} (°)	$\sigma_{water\ level}$ (m)
Scenarios 1 to 5	10.4	2.4	2.4	4.2	-
Scenarios 6 to 10	10.4	2.4	2.4	4.2	1.2

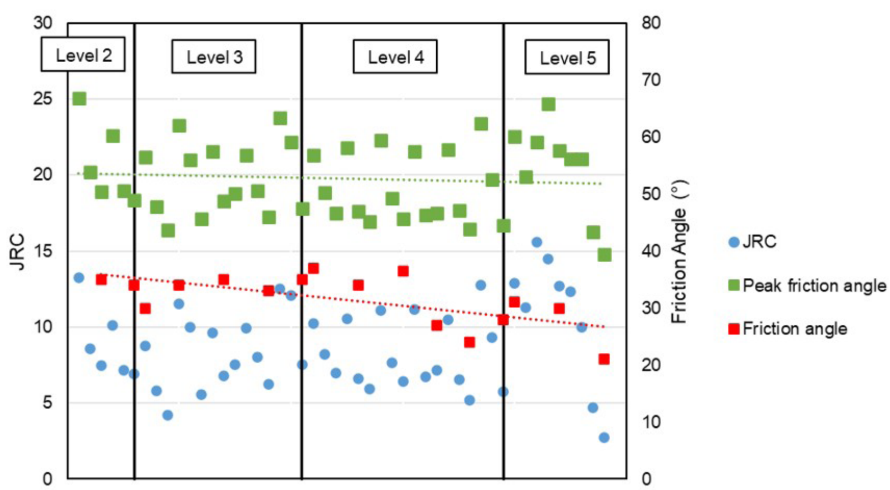

Figure 4. Dispersion of the *JRC* values, the peak friction angle, and the friction angle.

(blue trajectory), as well as two trajectories using *JCS* and ϕ values identical to the first two trajectories but altering only the *JRC* values to 10 and 0.5 (red and black trajectories, respectively). These *JRC* values were chosen to encompass a broader range of data points, aligning with values typically available in studies on the subject.

It is discernible from Figure 5 that the peak shear stress values are higher and, in general, lie within the range delineated by the trajectory based on intact joints (green) and highly altered joints (blue). Conversely, the ultimate shear stress values fall within the bounds of trajectories with *JRC* values of 10 (red) and 0.5 (black), with most of them situated below the blue trajectory (representing joints with a higher level of alteration).

This disparity primarily arises due to the pivotal role played by roughness in the initial shear resistance of these geological structures. Following the peak resistance, roughness assumes a diminishing role, consequently reducing the shear resistance of the samples.

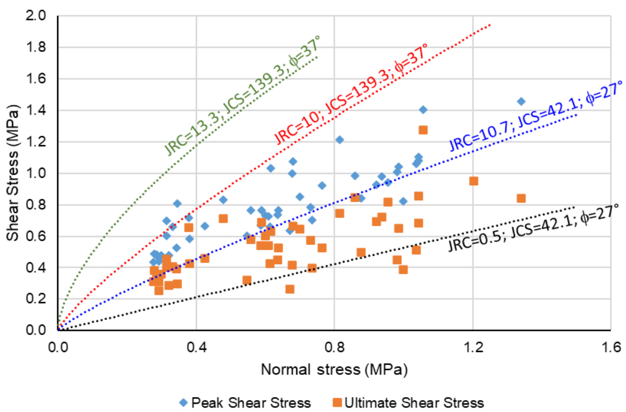

Figure 5. Peak and ultimate shear stress by normal stress and strength envelopes estimated by the Barton-Bandis model for parameters obtained in the laboratory.

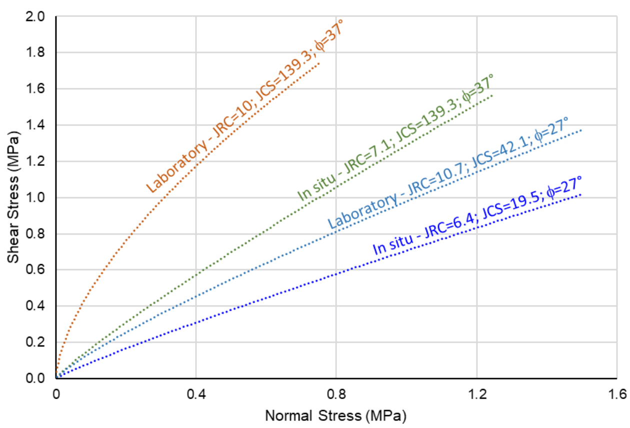

Figure 6. Strength envelopes by the Barton-Bandis model for laboratory and field parameters.

When employing field-derived parameters estimated through correlation with laboratory values, the trajectories become even more pronounced, as depicted in Figure 6.

As observed in Figure 6, the field trajectories exhibit a shallower slope when compared to the laboratory curves. As previously discussed, the smaller the tested specimen, the greater the influence of joint roughness on its shear resistance. Furthermore, it is evident from the trajectories of the intact rock, both for the laboratory (orange) and field (green), that the JRC value exerts a significant influence on the stress trajectories.

6.2 Deterministic stability analyses

Deterministic stability analyses were conducted using the Barton-Bandis criterion, considering the geometry and parameters defined in Section 5. The simulations were executed with Rocscience Slide2 software, employing the Spencer and Morgenstern-Price (GLE) methods for non-circular surfaces. The results obtained from the stability analyses are presented in Table 5.

Table 5. Safety Factors – *SF*.

Scenarios	Spencer	GLE
Scenario 1	2.82	2.80
Scenario 2	1.94	1.93
Scenario 3	1.74	1.74
Scenario 4	1.58	1.57
Scenario 5	1.46	1.45
Scenario 6	2.76	2.74
Scenario 7	1.89	1.88
Scenario 8	1.69	1.69
Scenario 9	1.53	1.52
Scenario 10	1.41	1.41

From the results presented in Table 5, a considerable reduction in the Safety Factor (*SF*) can be observed with an increasing level of alteration, for field-derived parameters.

Considering the field scenarios, the percentage reduction in *SF* becomes even more substantial, with the difference between Scenario 1 and Scenario 5 being approximately 48% and between Scenario 6 and Scenario 10, 49%.

It is important to highlight that between scenarios that used parameters for intact joints (Scenario 1 and 6) and those that used parameters for slightly altered joints (Scenario 2 and 7), there was a reduction in *SF* of approximately 31% for field scenarios. This significant decrease demonstrates that even for low levels of alteration, the rock mass strength can be considerably affected.

Regarding the water level in the sections, a reduction in *SF* ranging from 2% to 4% is observed for all scenarios considered in this study.

It should be noted that for field scenarios, joint alteration reduced the safety factors to values below 1.5, a threshold that may not be acceptable depending on the type of construction, as per Brazilian standards.

Furthermore, Lopes (2019) demonstrated that joints subjected to 8300 hours of accelerated percolation, according to Salles (2013), exhibit characteristics similar to those of naturally altered joints over a period of 10 years. Thus, a reduction of approximately 50% in *SF* for naturally altered samples over a decade represents a very significant decrease in strength, potentially leading to the failure of these altered slopes.

6.3 Probabilistic analyses

This chapter presents the results obtained from probabilistic analyses conducted using the First Order Second Moment (FOSM) and Monte Carlo methods. The equilibrium limit methods and configurations used for deterministic analyses remained consistent; therefore, simulations were executed using the Spencer and Morgenstern-Price (GLE) methods for non-circular surfaces, employing the Barton-Bandis model.

6.3.1 FOSM analyses

As discussed in the literature review, the First Order Second Moment (FOSM) method allows for the determination of the standard deviation of the *SF* (Safety Factor) function and its corresponding reliability index (β), thereby obtaining failure probability (*Pr*). To achieve this, the method calculates the *SF* variance by varying each parameter while keeping the others fixed.

Following Dell'Avanzi (1995) recommendation, a ±10% variation was employed for each parameter value. For scenarios without a water table, four parameters were considered variable: *JCS*, *JRC*, ϕ and γ. In contrast, for scenarios with a water table, five parameters were considered variable: *JCS*, *JRC*, ϕ, γ and *water level*.

In accordance with Vecci (2018, 2023), the fixation or lack thereof the critical failure surface has a relatively minor impact on failure probability in a problem analyzed by FOSM. Therefore, this study adopted the assumption of a free failure surface (without fixation).

From the *SF* values obtained for each parameter variation, the variance and standard deviation of the safety factor were calculated for each scenario, yielding the values of β and *Pr*. Table 6 presents the results obtained from the FOSM analyses for each of the scenarios, using the Spencer and GLE methods.

It is evident that for both the Spencer and Morgenstern-Price methods, for field scenarios considering parameters for intact joints (Scenarios 1 and 6) exhibit failure probability close to 5%.

The failure probability increases as the level of alteration increases and a significant increase in the failure probability can be observed between Scenarios 1 and 5, as well as between Scenarios 6 and 10.

As aforementioned, the FOSM method allows for the quantification of the relative contribution of each parameter to the failure probability calculated by the method. This application provides engineers with greater sensitivity to the problem and the most influential parameters, thereby guiding more effective engineering solutions.

Table 7 provides a summary of the relative contribution of each random variable to the variance of *SF* for each of the scenarios analyzed using the FOSM method, specifically for the Morgenstern-Price method.

From the results presented in Table 7, it can be observed that *JRC* is the parameter with the greatest influence on *SF* for the configuration analyzed in this study, followed by ϕ

Table 6. Results obtained in the FOSM analyses.

Scenarios	Spencer			GLE		
	SF	β	*Pr* (%)	*SF*	β	*Pr* (%)
Scenario 1	2.815	1.66	4.86	2.804	1.63	5.12
Scenario 2	1.939	1.56	5.97	1.931	1.57	5.87
Scenario 3	1.740	1.42	7.75	1.735	1.40	8.14
Scenario 4	1.578	1.27	10.18	1.572	1.26	10.45
Scenario 5	1.459	1.11	13.27	1.452	1.12	13.16
Scenario 6	2.757	1.61	5.33	2.743	1.61	5.41
Scenario 7	1.887	1.52	6.44	1.880	1.52	6.45
Scenario 8	1.691	1.36	8.76	1.685	1.34	8.95
Scenario 9	1.525	1.21	11.25	1.519	1.17	12.12
Scenario 10	1.411	1.02	15.46	1.405	1.02	15.28

Table 7. Percentage influence of each parameter on *SF* variation – GLE.

Scenario	*JCS*	*JRC*	γ	ϕ	*Water Level*
Scenario 1	0.1	82.6	0.1	17.2	-
Scenario 2	0.5	78.1	0.1	21.3	-
Scenario 3	0.7	77.2	0.1	22.0	-
Scenario 4	1.6	75.0	0.1	23.3	-
Scenario 5	3.4	71.3	0.2	25.1	-
Scenario 6	0.1	82.7	0.1	17.1	0.0
Scenario 7	0.4	78.4	0.0	21.1	0.1
Scenario 8	0.6	78.0	0.0	21.3	0.1
Scenario 9	1.7	75.5	0.0	22.7	0.1
Scenario 10	3.6	72.9	0.0	23.4	0.1

Table 8. Results from the analyses conducted using the Monte Carlo method. – GLE.

Scenario	SF_{det}	SF_{avg}	RI_{normal}	$RI_{lognormal}$	Pr (%)
Scenario 1	2.804	2.857	2.377	3.774	0.0
Scenario 2	1.931	2.044	1.720	2.314	0.4
Scenario 3	1.735	1.825	1.561	1.978	1.8
Scenario 4	1.572	1.637	1.401	1.672	3.6
Scenario 5	1.452	1.509	1.288	1.469	7.2
Scenario 6	2.743	2.800	2.338	3.678	0.0
Scenario 7	1.880	1.996	1.675	2.224	0.6
Scenario 8	1.685	1.779	1.504	1.877	2.3
Scenario 9	1.519	1.587	1.330	1.556	5.3
Scenario 10	1.405	1.463	1.213	1.354	9.9

and *JCS*. For the modeled problem, unit weight and water level exhibited no significant influence on the variance of *SF*.

Furthermore, it is noticeable that as the level of alteration increases, the influence of *JRC* decreases, while that of ϕ and *JCS* increases. This phenomenon aligns with the information presented in Figure 5, where a variation of JRC on the order of 3.3 (green and red curves) appears to have generated a greater reduction in strength than a variation on the order of 10.2 (blue and black curves).

6.3.2 Monte Carlo method analyses

Due to the significant computational effort required by the Monte Carlo method, this study opted to utilize Rocscience Slide2 software, which already incorporates the method in its statistical analysis options.

According to Silva (2015), in a normal distribution, approximately 99% of the sampling is covered when considering three standard deviations for each parameter. However, based on the mentioned value, the JRC value would become negative or exceed 20. Therefore, this study adopted the use of two standard deviations for each parameter. For Field Scenarios 5 and 10, only one standard deviation was employed to ensure that the *JCS* value did not become negative. Similar to the FOSM method, the assumption of a free failure surface, with no fixation, was maintained. The “overall slope” option was used, conducting the search for all possible probabilistic surfaces.

Table 8 presents the results obtained from the Monte Carlo method analyses for each of the field scenarios, using the Morgenstern-Price method.

As presented in Table 8, the failure probability for Scenarios 1 and 6 is zero and increases as the level of alteration rises, reaching 7.2% for Scenario 5 and 9.9% for Scenario 10.

The reliability index values, and failure probability obtained by the Spencer and Morgenstern-Price methods are consistent with each other for both probabilistic analysis methods.

Generally, the reliability index obtained by FOSM has values lower than those obtained by the Monte Carlo method. However, it can be observed that the magnitude of values obtained by FOSM is generally consistent with those obtained by Monte Carlo, especially when compared to the RI obtained through normal distribution.

Regarding the failure probability, the FOSM method yielded values higher than those obtained by Monte Carlo, which was expected as the latter method is more rigorous. For Field Scenarios 1 and 6, the failure probability calculated by FOSM was approximately 5%, while for Monte Carlo, it was zero. For Scenarios 5 and 10 (more altered), the difference in the PR percentages was also on the order of 5%, with values ranging from approximately 13% to 15% for FOSM and 7% to 10% for Monte Carlo.

Despite the differences, the use of the FOSM method for probabilistic analysis can be considered more interesting than Monte Carlo, as the associated error is not very high, and it allows engineers to identify which random variables have the greatest influence on the studied problem, thereby providing better guidance for engineering solutions.

7. Conclusion

The assessment of the alteration of rock materials in the study of geomechanical behavior of rock masses is of utmost importance and necessity. This work aimed to evaluate the influence of the alteration of gneiss joints on the stability and safety of the rock slopes at the Simplicio Hydroelectric Power Plant.

Regarding the results obtained in the parameterization of gneiss joints at different levels of alteration, the main conclusions are as follows:

i. A trend of reducing the friction angle with an increase in the level of joint alteration and an increase in result dispersion for more significant alteration levels was observed.

ii. For the peak friction angle, there is a less significant reduction trend, but the increased result dispersion for more altered samples led to an increase in the average peak friction angle for samples with a higher level of alteration.

iii. The JRC value obtained for each level of alteration underwent a slight initial reduction with a significant increase for moderately altered joints, along with increased dispersion.

iv. The dispersion of results is associated with the number of samples tested by direct shear, considered below the ideal.

v. Peak shear stress values are higher than ultimate shear stress values. This difference mainly arises due to the influence of joint roughness on joint strength at the onset of shearing. After the peak strength, the influence of roughness is less significant, as the irregularities rupture, reducing the shear strength of the samples.

vi. For field parameters obtained using the Barton & Choubey (1977) Method, the stress trajectories exhibit less inclination when compared to laboratory curves. This is a result of the sample size, as larger samples experience less influence from joint roughness on shear strength.

vii. The stress trajectories for intact and altered rock substantiate the significant influence of JRC values.

As for the results of deterministic analyses, the following conclusions can be drawn:

i. Safety Factor (*SF*) undergoes a considerable reduction with an increase in the level of alteration.

ii. For field scenarios, the percentage reduction in *SF* is even greater, reaching 50% when comparing scenarios with intact joints to the scenario with the most altered joints.

iii. Considering the water level in the sections led to a reduction in *SF* ranging from 2% to 4% for all scenarios in this study.

iv. For field scenarios, joint alteration reduced the safety factors to values below 1.5.

v. The results indicate a reduction of approximately 50% in *SF* for naturally altered samples over a decade, representing a very significant decrease in strength, which can lead to the failure of altered slopes.

The results obtained from the probabilistic analyses allow us to conclude that:

i. For scenarios considering intact joint parameters, the FOSM method provided a failure probability close to 5% for field scenarios.

ii. With the FOSM method, the failure probability increases as the level of alteration of the samples increases.

iii. In the FOSM method, *JRC* is the parameter with the most influence on the *SF* for the configuration analyzed in this research, followed by the friction angle and *JCS*. Unit weight and water level have no significant influence on *SF* variance.

iv. In the FOSM method, the influence of *JRC* decreases with an increase in the level of alteration, while the influence of the friction angle and *JCS* increases.

v. Both FOSM and Monte Carlo methods indicate a significant increase in the failure probability between field scenarios with intact joints and moderately altered joints.

vi. The reliability index and failure probability obtained with the Spencer and Morgenstern-Price methods are convergent.

vii. The reliability index obtained by FOSM has values lower than those obtained by the Monte Carlo method, but the values are of the same order of magnitude, especially when compared to the reliability index obtained through normal distribution.

viii. Regarding the failure probability, the FOSM method provides values higher than those of Monte Carlo.

ix. For scenarios with intact joints, the failure probability calculated by FOSM is 5%, while for Monte Carlo, it is zero. For moderately altered scenarios, the difference between the PR percentages is also 5%, with values ranging from approximately 13% to 15% for FOSM and 7% to 10% for Monte Carlo.

x. The use of the FOSM method for probabilistic analysis can be considered more advantageous than Monte Carlo, as its associated error is not very high, and it allows engineers to identify which random variables have a greater influence on the studied problem, leading to more precise engineering solutions.

Acknowledgements

The authors gratefully acknowledge the financial support of the Coordenação de Aperfeiçoamento de Pessoal de Nível Superior – Brasil (CAPES) and the Conselho Nacional de Desenvolvimento Científico e Tecnológico – Brasil (CNPq).

Declaration of interest

The authors have no conflicts of interest to declare. All co-authors have evaluated the paper contents in detail and there are no financial advantages and no conflicts of interest to declare.

Authors' contributions

Patrícia Martins Lopes: conceptualization, data curation, formal analysis, investigation, software, writing - original draft. Alberto de Sampaio Ferraz Jardim Sayão: methodology, supervision, validation, visualization, writing – review & editing. Anna Laura Lopes da Silva Nunes: data curation, methodology, resources, supervision, validation, visualization, writing – review & editing.

Data availability

The datasets generated analyzed in the current study are available by the corresponding author upon request.

List of symbols

c_j	Cohesion intercept of the joint
c	Cohesion intercept
i	Average angle of deviation of particle displacements from the direction of the applied shear stress.
JCS	Joint Compressive Strength
JCS_n	JCS extrapolated to in situ sample size
JCS_o	JCS measured in the laboratory
JRC	Joint Roughness Coefficient
JRC_n	JRC extrapolated to in situ sample size
JRC_o	JRC measured in the laboratory
L_n	Joint in situ length
L_o	Joint length in laboratory
R	Rebound number
γ	Dry unit weight of rock
σ_n	Effective normal stress
σ_C	Uniaxial compression strength
τ	Peak shear strength
ϕ_b	Basic friction angle
ϕ_r	Residual friction angle
ϕ	Friction angle

References

Assis, A.P., Barbosa, T.J.E., Almeida, M.G.G., & Maia, J.A.C. (2018). *Métodos estatísticos e probabilísticos aplicados a geotecnia (handout)*. Programa de Pós-graduação em Geotecnia, Departamento Engenharia Civil e Ambiental, Universidade de Brasília - UNB (in Portuguese).

Bandis, S. (1980). *Experimental studies of scale effects on shear strength, and deformation of rock joints* [Doctoral thesis, University of Leeds]. University of Leeds.

Barton, N. (1973). Review of a new shear-strength criterion for rock joints. *Engineering Geology*, 7(4), 287-332. http://doi.org/10.1016/0013-7952(73)90013-6.

Barton, N.R. (1978). Rock mechanics review: the shear strength of rock and rock joints. *International Journal of Rock Mechanics and Mining Sciences & Geomechanics Abstracts*, 13(9), 255-279. http://doi.org/10.1016/0148-9062(76)90003-6.

Barton, N.R., & Bandis, S. (1982). Effect of block size on the shear behavior of jointed rocks. In *Proceedings of the Symposium on Rock Mechanics* (pp. 739-760). Berkeley: AIME.

Barton, N., & Choubey, V. (1977). The shear strength of rock joints in theory and practice. *Rock Mechanics*, 10(1), 1-54. http://doi.org/10.1007/BF01261801.

Barton, N.R., Wang, C., & Yong, R. (2023). Advances in joint roughness coefficient (JRC) and its engineering applications. *Journal of Rock Mechanics and Geotechnical Engineering*, 15(12), 3352-3379. http://doi.org/10.1016/j.jrmge.2023.02.002.

Christian, J.T., Ladd, C.C., & Baecher, G.B. (1992). Reliability applied to slope stability analysis. *Journal of Geotechnical Engineering*, 120(12), 2180-2207. http://doi.org/10.1061/(ASCE)0733-9410(1994)120:12(2180).

Dantas Neto, S.A., Albino, M.C., Leite, A.R.S., & Abreu, A.A. (2022). Development of neuro-fuzzy models for predicting shear behavior of rock joints. *Soils and Rocks*, 45(4), 1-13. http://doi.org/10.28927/SR.2022.003322.

Dehler, N. M., & Machado, R. (2002). Geometria e cinemática da aba sul da estrutura divergente do Rio Paraíba do Sul ao longo da seção Areal-Três Rios, Rio de Janeiro. *Revista Brasileira de Geociências*, 32(4), 481-490. http://doi.org/10.25249/0375-7536.2002324481490.

Dell'Avanzi, E. (1995). *Confiabilidade e probabilidade em análises de estabilidade de taludes* [Master's dissertation]. Pontifícia Universidade Católica do Rio de Janeiro (in Portuguese).

Goodman, R.E. (1970). The deformability of joints. In *Proceedings of the Determination of the in-Situ Modulus of Deformation of Rock* (pp. 174-196). Denver. ASTM International. http://doi.org/10.1520/STP29147S.

Griffiths, D.V., & Fenton, G.A. (2007). *Probabilistic methods in geotechnical engineering*. International Centre for Mechanical Sciences. http://doi.org/10.1007/978-3-211-73366-0.

Guidicini, G., & Nieble, C.M. (1983). *Estabilidade de taludes naturais e de escavação* (2. ed.). Editora Blucher.

Kveldsvik, V., Nilsen, B., Einstein, H. H., & Nadim, F. (2008). Alternative approaches for analyses of a 100,000 m3 rock slide based on Barton–Bandis shear strength criterion. *Landslides*, 5, 161-176. https://doi.org/10.1007/s10346-007-0096-x.

Leite, A.R.S., & Dantas Neto, S.A. (2020). A predictive model for the peak shear strength of infilled soft rock joints developed with a multilayer perceptron. *Soils and Rocks*, 43(4), 575-589. http://doi.org/10.28927/SR.434575.

Lopes, P.M. (2019). *Alterability and geomechanical behavior of rocks at AHE Simplício* [Master's dissertation]. Universidade Federal do Rio de Janeiro – COPPE/UFRJ (in Portuguese). http://hdl.handle.net/11422/14017

Lopes, P.M. (2023). *Slope stability at Simplicio Hydroelectric Complex due to alteration of rocky material* [Doctoral thesis]. Pontifícia Universidade Católica do Rio de Janeiro – PUC-Rio (in Portuguese).

Machado, D.L. (2012). *Geomechanical behaviour of relict structures of a residual soil of gneiss on AHE Simplício*.

[Master's dissertation]. Universidade Federal do Rio de Janeiro – COPPE/UFRJ (in Portuguese).

Maia, P.C.A. (2001). *Evaluation of the geomechanical behavior and the alterability of rockfills* [Doctoral thesis]. Pontifícia Universidade Católica do Rio de Janeiro – PUC-Rio (in Portuguese). http://doi.org/10.17771/PUCRio.acad.2075.

Maia, P.C.A., Sayão, A.S.F.J., Nunes, A.L.L.S., & Caproni Junior, N. (2002). Compressibilidade de enrocamentos basálticos. In *Proceedings of the XXIV Seminário Nacional de Grandes Barragens* (Vol. 2, pp. 81-92). Fortaleza.

Maia, P.C.A., Sayão, A.S.F.J., & Nunes, A.L.L.S. (2003). Considerações sobre a alteração de enrocamentos. *XXV Seminário Nacional de Grandes Barragens*, 1(T91), 214-228.

Marchesi, V.R. (2008). *Modelagem geomecânica tridimensional de maciços rochosos para análise bidimensional da estabilidade dos taludes de escavação da casa de força do AHE-Simplício* [Master's dissertation]. Pontifícia Universidade Católica do Rio de Janeiro – PUC-Rio (in Portuguese).

Marinho, C.A.S. (2007). *Estudos geológicos-geotécnicos do AHE Simplício* [Undergraduate thesis]. Universidade Federal Rural do Rio de Janeiro (in Portuguese).

Motta, C., Capellão, S.L.F., Borges, J.B., Ortega, M.C., & Moraes, R.B. (2009). Simplício Hydroelectric Project on the Paraíba do Sul River. In Brazilian Committee on Dams. *Main Brazilian Dams III: design, construction and performanc*e (pp. 411-436). Brazilian Committee on Dams.

Oliveira, J.R. (2017). *Classification and strength of fresh and weathered rock joints* [Master's dissertation]. Universidade Federal do Rio de Janeiro – COPPE/UFRJ (in Portuguese).

Patton, F. D. (1966). Multiple modes of shear failure in rock. In *International Society for Rock Mechanics and Rock Engineering.* Lisbon: ISRM.

Pratt, H., Black, A., & Brace, W. (1974). Friction and deformation of jointed quartz diorite. In *Proceedings of the 3rd Congress of ISRM* (pp. 306-310). Denver. ISRM.

Press, F., Siever, R., Grotzinger, J., & Jordan, T.H. (2006). *Para entender a terra* (4. ed.). Bookman.

Salles, R.O. (2013). *Alterabitity and geomechanical behavior of the gneiss of Simplício's Hydroelectric Power Plant* [Doctoral thesis]. Universidade Federal do Rio de Janeiro – COPPE/UFRJ (in Portuguese).

Sayão, A.S.F.J., Sandroni, S.S., Fontoura, S.A.B., & Ribeiro, R.C.H. (2012). Considerations on the probability of failure of mine slopes. *Soils and Rocks*, *35*(1), 31-37. http://doi.org/10.28927/SR.351031.

Silva, C.C. (2015). *Análise de estabilidade de um talude da cava de Alegria utilizando abordagem probabilística*. [Master's dissertation]. Universidade Federal de Ouro Preto – UFOP. http://www.repositorio.ufop.br/jspui/handle/123456789/6375

Steffens, A.H.D. (2018). *Strength of natural and artificially weathered rock joints* [Master's dissertation]. Universidade Federal do Rio de Janeiro – COPPE/UFRJ (in Portuguese).

Teixeira, W., Toledo, C., Fairchild, T., & Taioli, F. (2000). *Decifrando a terra*. Oficina de Textos (in Portuguese).

Valeriano, C. M. (2006). *Reconhecimento Geológico-Estrutural da Área do AHE Simplício (RJ)*. Technical report (in Portuguese).

Vecci, A.N. (2018). *Probabilistic analysis of a mine slope stability* [Master's dissertation]. Pontifícia Universidade Católica do Rio de Janeiro (in Portuguese). http://doi.org/10.17771/PUCRio.acad.35100.

Vecci, A.N. (2023). *Probabilistic assessment methodology of geotechnical constructions* [Doctoral thesis]. Pontifícia Universidade Católica do Rio de Janeiro (in Portuguese).

Viana, L.L. (2010). *Individualização de orto e paragnaisses que ocorrem no sítio de obras do AHE Simplício Queda – Única, Rio de Janeiro, RJ* [Undergraduate thesis]. Universidade Federal Rural do Rio de Janeiro (in Portuguese).

Woo, I., Fleurisson, J.A., & Park, H.J. (2010). Influence of weathering on shear strength of joints in a porphyritic granite rock mass in Jechon area, South Korea. *Geosciences Journal*, 14(3), 289-299. http://doi.org/10.1007/s12303-010-0026-0.